JOURNAL OF CATALYSIS 29, 374–384 (1973)

Structure and Surface Properties of Supported Platinum Catalysts

P. RATNASAMY, A. J. LEONARD, L. RODRIQUE,*
AND J. J. FRIPIAT

Laboratoire de Physico-Chimie Minérale, Institut des Sciences de la Terre, de Croylaan, 42, 3030 Heverlee, Belgium

Received June 6, 1972

Supported Pt catalysts characterized by various dispersion degrees and Pt contents in the range 0.5–0.8% have been studied by the Radial Electron Distribution (RED) technique. Also two catalysts richer in Pt (1.4–2.9%) have been examined by electron microscopy and microprobe. The RED reveals two peaks obviously due to Pt, i.e., Pt–Pt_1 and Pt–Pt_2 at 2.75 ± 0.05 Å and 3.94 ± 0.07 Å, respectively. These interatomic distances compare well with those observed in f.c.c. bulk platinum at 2.774 Å and 3.923 Å. The dispersion degree measured by the titration (Benson and Boudart) technique, has been related in a semiquantitative manner to the intensity of the RED peak corresponding to the Pt–Pt_1 distance, i.e., 2.75 Å, and a model for a Pt particle is proposed. Such an "average" particle is composed of n_u unperturbed layers of Pt atoms with coordination number Z = 12 and of n_p perturbed external layers. In order to reconcile the average radius obtained from electron micrographs with the degree of dispersion, it must be assumed that the number of perturbed layers is about 2.

In the perturbed layers of Pt catalysts prereduced and then exposed to the atmosphere, the average coordination number of the Pt atom is very low (almost zero), suggesting a complete disorder provoked most probably by the introduction of oxygen atoms. For catalysts reduced inside the RED camera and thus not exposed to the atmosphere, the coordination number of Pt atoms in the perturbed layers is about $Z/2 = 6$, suggesting that the remaining hydrogen atoms are in the holes between Pt atoms.

INTRODUCTION

Platinum, finely dispersed on high surface-area oxides like alumina or silica–alumina is widely used as a catalyst for many reactions. In recent years, many diverse techniques have been used to elucidate the nature and structure of platinum in these catalysts (*1*). Information concerning the degree of dispersion of platinum, the size and shape of the metal crystallites, the oxidation state of the platinum atoms, the predominant faces of the platinum crystallites that are exposed, and the Pt–Pt distances are highly desirable for a rational interpretation of the activity of these catalysts. Since many supported platinum catalysts are highly amorphous, structural information concerning them cannot be obtained by such classical techniques as X-ray and electron diffraction. This explains why almost all the structural data about commercial platinum catalysts have been derived from adsorption measurements (H_2 or $H_2 + O_2$), X-ray line broadening or electron microscopic techniques. All the three provide information concerning the dispersion of platinum on the surface of the support as well as the crystallite size of the metal particles. There is hardly any information

* M.R.A.C., Tervuren.

available on the Pt–Pt distances. Recently the method of Radial Electron Density (RED) distribution has been applied to many amorphous catalysts (*2*). This is one of the techniques most suited to obtain information about interatomic distances in amorphous materials.

In the present study, this technique has been extended to platinum/alumina and platinum/silica–alumina catalysts. Hydrogen adsorption, electron microscopy and electron probe analysis have been used to deduce the degree of dispersion of platinum. This structural information reveals a more detailed picture of the surface of supported platinum catalysts.

Experimental Methods

1. Materials

The supported platinum catalysts were obtained from various commercial sources and their main structural and surface properties are compiled in Table 1. The platinum dispersion was obtained according to the procedure proposed by Benson and Boudart (*3*): the stoichiometry adopted by these authors corresponds to the consumption of 3 H per Pt atom. The catalysts were reduced in a flow (4 liter/hr) of pure and dry H_2 for 8 hr at 400°C before use. In most of the runs they were exposed to the air either for a short time (electron microscopy and electron probe) or for several hours (radial electron distribution).

Therefore, a RED camera was built in which the catalyst could be reduced before the run and kept under an H_2 atmosphere during the run.

Unfortunately the camera alignment, which is an extremely critical factor in the RED technique, was very difficult to maintain in the high temperature attachment.

It is for this reason that no more than four samples have been studied in that way.

2. Methods

The X-ray scattering technique used in the radial electron distribution (RED) as well as the method for calculating the

TABLE 1
Structural and Surface Properties of the Catalysts

Code[b]	wt% Pt	Support	% Dispersion (D)	$\Delta\rho_0$[a]	$\Delta\rho_r$[a]	r(Pt–Pt$_1$) (Å)	r(Pt–Pt$_2$) (Å)
254/063B	0.547	silica-alumina	10.44	1393		2.80	4.12
254/063A	0.539	silica-alumina	11.44	948		2.74	3.88
254/099A	0.795	silica-alumina	12.67	872	1964	2.64 (2.77)	4.04 (3.99)
254/032A	0.671	silica-alumina	19.40			2.74	3.88
254/035A	0.760	silica-alumina	34.57			2.74	3.86
81/059A	0.772	silica-alumina	46.27	328		2.74	3.92
254/099B	0.759	silica-alumina	51.20	545	1525	2.80 (2.76)	4.03 (3.98)
81/059C	0.731	silica-alumina	51.93	518		2.63	3.91
81/059B	0.759	silica-alumina	60.45	443		2.76	3.97
254/032B	0.662	silica-alumina	77.36	350		2.74	3.81
10/336C	2.939	silica-alumina	55.47	used for electron microscopy			$\langle\rho C\rangle$ = 12.6 Å
10/336B	1.438	silica-alumina	68.13	used for electron microscopy			$\langle\rho C\rangle$ = 12.0 Å
254/103A	0.639	alumina	20.80	773	1364	2.84 (2.75)	3.97 (4.02)
254/103B	0.748	alumina	78.13	209	799	2.78 (2.73)	3.86 (4.05)
			Average interatomic distances			2.75 (2.75) ±0.05 (0.01)	3.94 (4.01) ±0.07 (0.03)

[a] $\Delta\rho_0$ and $\Delta\rho_r$ are the differential amplitudes of the RED peaks observed at 2.75 A for the prereduced catalyst and the catalyst reduced *in situ*. The radii between brackets are those observed for the catalyst reduced *in situ*.

[b] The catalysts were supplied by LABOFINA BRUSSELS.

RED patterns and their significance have already been described in detail (*2*).

For the electron microscopic study, the samples were first ground in a mortar and then dispersed in distilled water. A drop of this suspension was deposited on a copper support grid of the AEI type (Smethurst Highlight Ltd.), covered with a thin carbon film and dried in a desiccator. For the microprobe analysis, the catalyst granules were directly put on the carbon film. No shadowing or coating was made in any case. A combined AEI EM 6G electron microscope–X-ray microanalysis attachment was used for electron optical and microprobe studies. An accelerating potential of 100 kV and a high contrast aperture of 25 μm diameter were used for bright field transmission microscopy.

For the microprobe analysis, the analyzer crystals were mica for Si$K\alpha$ and Al$K\alpha$ and LiF for Pt$L\alpha_1$. The accelerating voltage of the electrons was 60 kV and the probe current, 0.08 A. The diameter of the probe was about 6 μm. The probe current was checked after each recording of the intensity ratios Pt/Al and Pt/Si.

These intensity ratios have been recorded on different granules as well as on different regions of the same granule. The impact of the electron beam on these insulating materials sometimes heated the samples sufficiently to cause the fusion of some grains. This is probably the origin of some of the abnormal results which were neglected in the calculation of the gaussian distributions.

Experimental Results

1. Platinum Dispersion and Crystallite Size

All catalysts have been submitted to X-ray diffraction (Cu$K\alpha$ radiation). Only sample 254/099 A produced any X-ray pattern. For this sample, the 111 reflection ($d_{111} = 2.254$ Å) was clearly visible. At first sight it is surprising that the other catalysts characterized by dispersion in the same range as that found for 254/099 A, i.e., about 10%, did not behave in the same way.

A possible explanation is that in the above example, a small fraction of platinum forms a few large particles responsible for the X-ray pattern and that these particles do not affect appreciably the degree of dispersion measured by the titradition technique. Even though the platinum contents of these catalysts differ by a factor of less than 2, the degree of dispersion D varies by a factor of more than 7, as shown in Table 1.

Electron microscopy could possibly throw more light on the Pt particle size distribution. Such a study has been possible for two catalysts richer in Pt than usual. Some representative results are illustrated in Fig. 1 which shows electron micrographs of dispersed particles from catalysts 366, B and C. It is clearly seen that the distribution of Pt particles is not uniform throughout the silica–alumina gel; the low-magnification micrograph shows that the Pt particles are much more concentrated in certain regions (see for example the surrounded area in Fig. 1a). Such regions from both catalysts have been used to calculate the crystallite size distribution by screening 500 crystallites in terms of their diameter for each catalyst. The crystallites were assumed to be spherical which in fact they appear to be. It should be mentioned that the values for the 10 Å range are less accurate than for other ranges.

As shown in Fig. 2, there is a marked difference in the particle size distributions for these two catalysts. However, the average radii are quite close to each other, i.e., 12 and 12.6 Å for catalysts 366, C and B, respectively.

In order to obtain more information on distribution profiles, an electron microprobe analysis of the same regions was carried out. The results are shown in Figs. 3 and 4. In these figures, the abscissa gives the ratio $r_i = I_{Pt}/I_{Si}$ (A and B) or I_{Pt}/I_{Al} (A′ and B′), that is the intensity of the radiation from platinum atoms (measured in Hz) to the intensity of the radiation from silicon or aluminium atoms. r_i is thus proportional to the Pt concentration. The ordinate is the gaussian distribution of

these r_i values according to

$$\omega(r_i) = \frac{1}{\sigma_r \sqrt{2\pi}} \exp - [(r_i - \bar{r})^2/2\sigma_r^2] \quad (1)$$

with the usual notation. About 20 readings were taken for each microprobe scanning. The distributions for sample 366 C are seen to be wider than that for 366 B, reflecting the wider distribution of the dimensions of the platinum crystallites in the former. The results from both electron microscopy and microprobe analysis are thus in agreement. They suggest that catalysts with larger amount of platinum (366 C as opposed to 366 B for instance) contain also larger crystallites even if the average radii are not noticeably different. Such a suggestion may be important since Anderson and Avery (4) have shown a dependence of the selectivity of supported platinum catalysts on the surface concentration of triplet sites whose density will

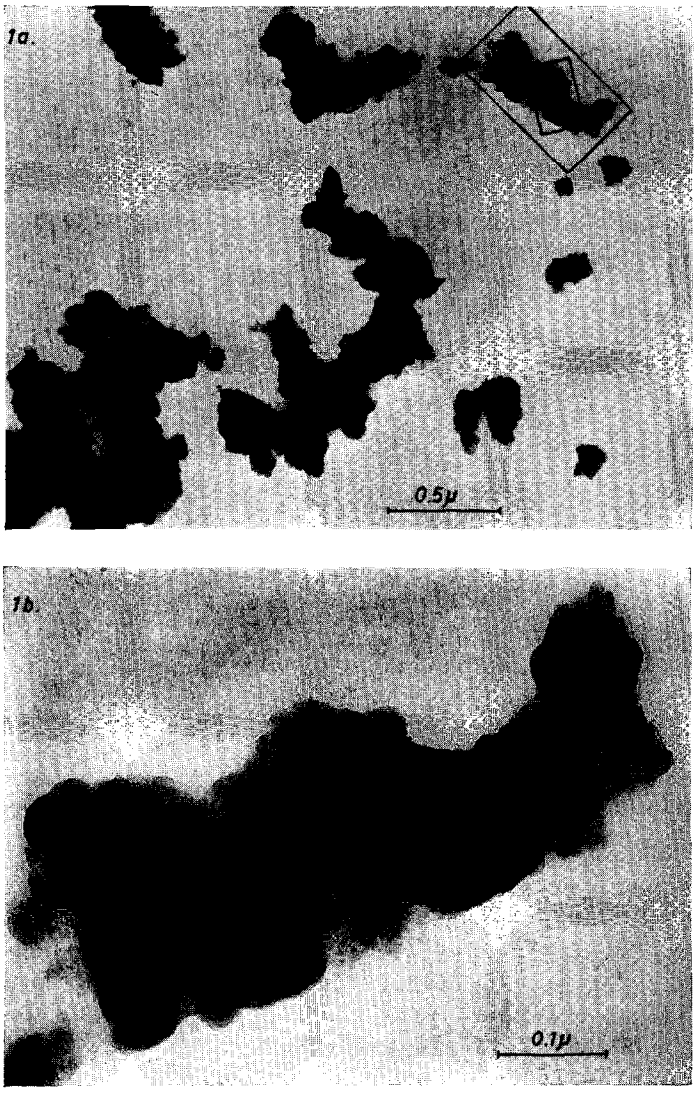

FIG. 1. (a) Electron micrograph from the 366C catalyst (×74,000). The upper right part of the micrograph shows particles of silica-alumina gel on which can be seen an agglomeration of Pt crystallites. (b, c) Enlargements of the surrounded areas in the first micrograph (×355,000 and ×790,000, respectively). (d) Electron micrograph from the 366B catalyst showing Pt crystallites dispersed in gel (×790,000).

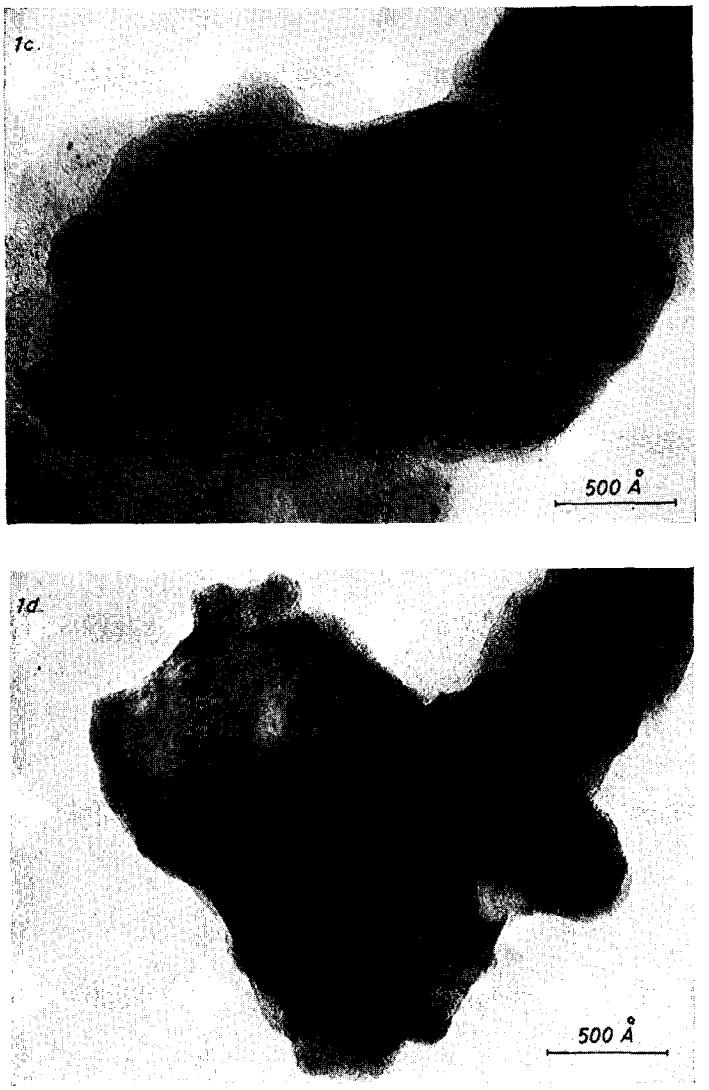

FIG. 1. (*Continued*)

be a sensitive function of the crystallite size.

2. Radial Electron Density Distribution (RED)

The RED patterns of all the catalysts listed in Table 1 have been studied. Because of an instrumental failure, the RED obtained for catalysts 062 A and 065 A do not have the semiquantitative character of the other results. As illustrative examples the RED patterns of two Pt/aluminas (103, A and B) and three Pt/silica–aluminas (062 A, 063 A and 065 A) as well as those of the corresponding supports are shown in Fig. 5. A detailed study of the structure of amorphous silica-aluminas similar to the supports used here has been published elsewhere (*5*).

The Pt–Pt interatomic distances are compiled in Table 1. The interatomic vectors corresponding to other atoms (Si, Al, O) are collected in Table 2. In platinum metal, which has a face centered cubic structure, the Pt–Pt_1 and Pt–Pt_2 distances are 2.774 Å (corner to center of face) and 3.923 Å (length of the edge), respectively. Considering the experimental errors, these

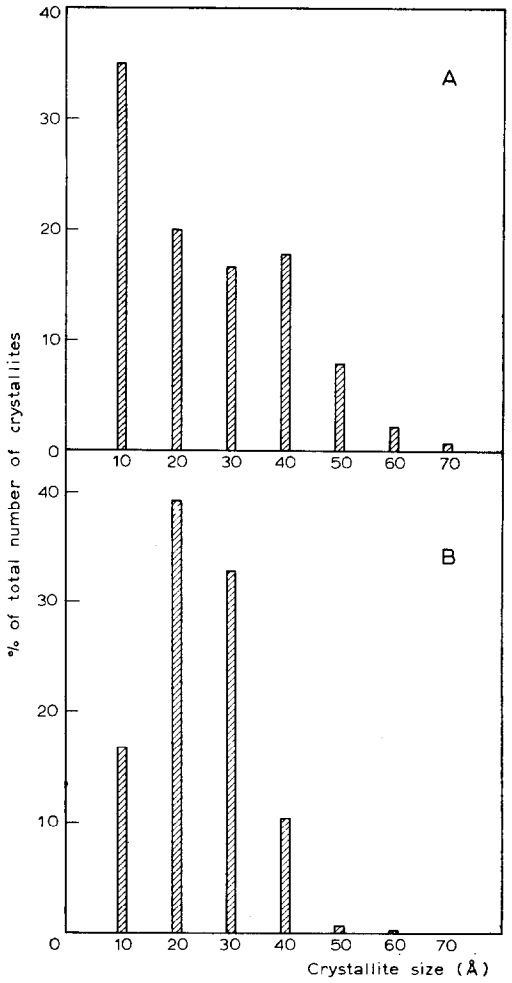

FIG. 2. Size distribution of platinum crystallites derived from high resolution electron micrographs for catalysts (A) 366C and (B) 366B.

distances are in good agreement with those derived from the RED peaks observed at 2.75 ± 0.05 Å and at 3.94 ± 0.07 Å, respectively.

The average distance observed after reduction *in situ* for Pt–Pt_2 is not within the right range, probably because of too few observations. Apparently both the observed Pt–Pt_1 and Pt–Pt_2 distances seem to be independent of the nature of support, total platinum content and dispersion. It should not be concluded, however, that around each platinum atom the distribution of neighboring Pt atoms is identical to that in bulk metal. The constancy of the Pt–Pt_1 and Pt–Pt_2 interatomic vectors just means that only those atoms at the right distances contribute to the corresponding RED peaks and the proof that an appreciable fraction of the Pt atoms does not contribute to these peaks results clearly from intensity measurements. If the RED function obtained for the support is subtracted from that observed for the catalyst in the region of the Pt–Pt_1 distance, the difference represents the contribution of this vector to the X-ray scattering. Figure 6 shows that these differences ($\Delta\rho$) are characteristic for a given catalyst.

Since a single RED peak is gaussian shaped, its amplitude ρ is related to its surface S as follows

$$\rho = S/1.064W_{hb} \qquad (2)$$

where W_{hb} is the half-height band width. For a specific Pt–Pt interatomic distance

$$\rho = K^2\nu \qquad (3)$$

where K represents the atomic number of platinum and where ν is the multiplicity of this interatomic vector, i.e., in the case of a homoatomic structure the coordination number associated with this distance. Therefore, ρ is proportional to ν. Since the amplitude is expressed as the differences between the RED functions for the supported Pt catalyst and for the very same support and that the RED function is not normalized for Pt but for the support composition, the difference $\Delta\rho$ is proportional to the total number of Pt–Pt vectors of a specified length, i.e.,

$$\Delta\rho \propto N \qquad (4)$$

where N is ν times the number of Pt atoms contributing to the RED peak. The values of $\Delta\rho_0$ for the prereduced catalysts and of $\Delta\rho_r$ for the catalysts reduced *in situ*, are listed in Table 1. There is obviously a correlation between $\Delta\rho_0$ and the dispersion. Moreover the amplitudes $\Delta\rho_r$ observed after reduction *in situ* are more intense than $\Delta\rho_0$.

It may thus be concluded that the number N of interatomic vectors contributing to a specified RED peak is a function of

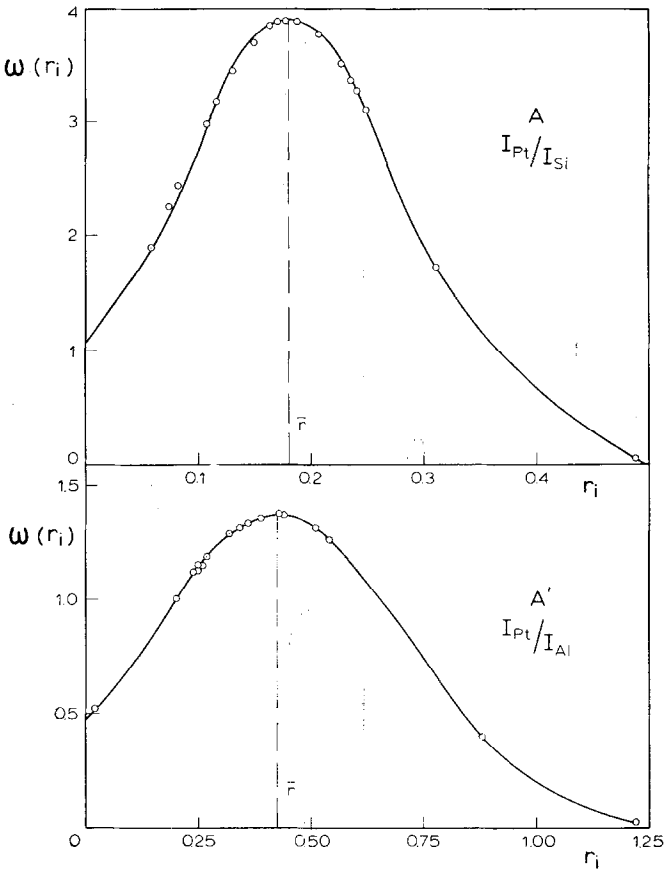

FIG. 3. Gaussian distribution of the Pt/Si and Pt/Al intensity ratios obtained by electron microprobe analysis for the 366C catalyst.

the dispersion degree and of the oxidation (or reduction) state of the Pt surface.

DISCUSSION

Let us assume that the Pt spherical particles are composed from a close packing of holes of identical radii $\rho = 1.39$ Å and let us consider that to a specified dispersion D corresponds a sphere of average radius $C\rho$ (Fig. 7). In region I, all the holes are permanently occupied by Pt atoms. The number of Pt atoms in these unperturbed concentric layers is $(2n_u + 1)^3$. In region II, for the prereduced catalyst which has been exposed to the air, the number of oxygen atoms is supposed to be equal to the number of Pt atoms in order to fit the Pt–O stoichiometry. Therefore in region II, made from n_p perturbed layers, the number of Pt atoms is $(1/2)$ $[(2n_u + 2n_p + 1)^3 - (2n_u + 1)^3]$. The radius of the sphere is of course $(2n_u + 2n_p + 1)\rho = C\rho$ and the so-called degree of dispersion D becomes

$$D = \frac{C^3 - (2n_u + 1)^3}{(2n_u + 1)^3 + C^3}. \qquad (5)$$

Per unit weight of a catalyst containing w percent Pt, the number of spherical Pt particles, assumed to be all alike, is $3w/(400\ C^3 d)$. For each of them, in region I, the number of interatomic Pt–Pt vectors (corresponding to the 2.774 Å distance) is $(2n_u + 1)^3 \times Z$, where Z is the Pt coordination number. In region II, this number is $(Z'/2)$ $[(2n_u + 2n_p + 1)^3 - (2n_u + 1)^3]$ where Z' is the coordination number in the n_p perturbed layers. Therefore per unit weight of Pt in the supported catalyst the number of interatomic Pt–Pt

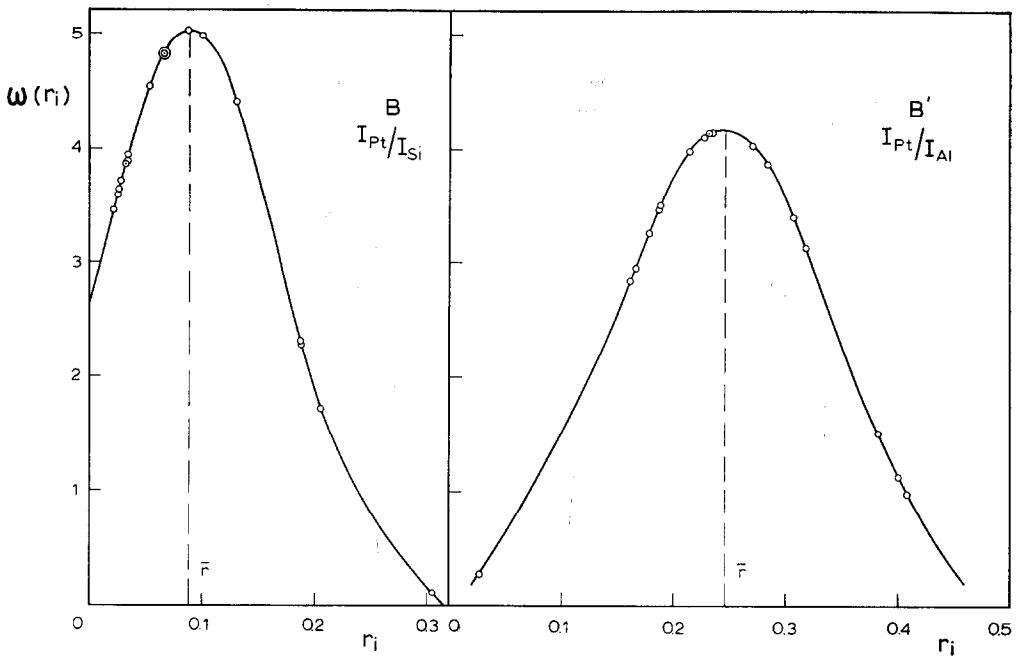

FIG. 4. Gaussian distribution of the Pt/Si and Pt/Al intensity ratios obtained by microprobe analysis for the 366B catalyst.

vectors is

$$N = \{Z(2n_u + 1)^3 + (Z'/2)[C^3 - (2n_u + 1)^3]\} \times 3w/400\pi C^3 d$$

and using Eq. (5), the number N of interatomic vectors in Eq. (4), becomes

$$N = \frac{3w}{400\pi d} \frac{Z - D(Z - Z')}{1 + D} \qquad (6)$$

where $Z' < Z$.

For the few samples that have been reduced a second time in the RED camera at 400°C, since the radius of the remaining H atoms in the perturbed layers is such as they can fit the holes between Pt atoms in close packing without perturbing appreciably the Pt–Pt interatomic distance, N' is

$$N' = \frac{3w}{400\pi d} \frac{Z - D(Z - Z'')}{1 + D}$$

where $Z'' > Z'$. Therefore $\Delta\rho_r/\Delta\rho_0$ should be equal to

$$N'/N = \frac{Z - D(Z - Z'')}{Z - D(Z - Z')} \qquad (7)$$

Equations (6 and 7) result of course from an oversimplified and crude treatment. In particular the border effects on the coordination number in the outside layers of regions I and II have been explicitly neglected. Actually, they are implicit in Z' or Z''. Nevertheless, the semiquantitative character of the RED method does not justify a more sophisticated treatment. Equation (5) can be easily checked, as shown in Fig. 8, by plotting D against ρC for various values of n_p and by introducing in this diagram the dispersion degrees and the average radii observed for samples 366, C and B (see Table 1). The two experimental points are in between the curves obtained for $n_p = 1$ and $n_p = 2$ but closer to the latter. As $\Delta\rho_0$ is proportional to N, the best way to check Eq. (6) is to plot $\log(\Delta\rho_0/w)$ vs $\log[Z - D(Z - Z')]/[1 + D]$ for various values of Z'. $Z = 12$ for a f.c.c. structure. The best agreement has been obtained for $Z' = 0$ and this correlation may be considered as quite reasonable as shown in Fig. 9, considering the semiquantitative character of the RED method. We do not pretend that Z' is exactly zero but it must

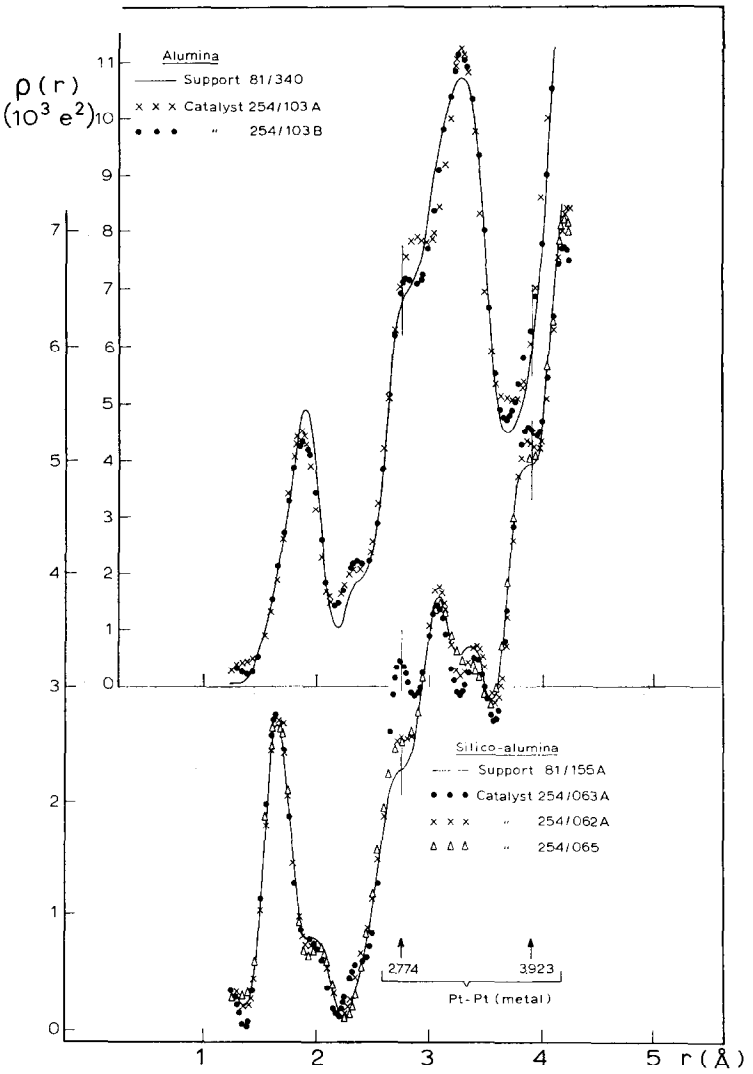

FIG. 5. Radial electron density distributions for catalysts 103A, 103B, 062A, 063A, and 065A. The solid lines represent the distributions for the alumina and silica-alumina supports, respectively.

be very low. This means that in the perturbed first or two first layers, the oxygen chemisorption by the prereduced catalyst introduced a complete disorder in the Pt atom distribution.

Finally, Eq. (7) has been tested by plotting $\log(\Delta\rho_r/\Delta\rho_0)$ against $\log[Z - D(Z - Z'')]/[Z(1 - D)]$ for various values of Z''. As shown in Fig. 9, the best fit with the experimental data has been obtained for $Z'' = Z/2$, as could be expected for surface layers. A crude but coherent representation of the platinum atom distribution emerges therefore from the simultaneous measurements of the dispersion degree by the titration technique and of the radial electron distribution completed by a few but careful electron microscopy investigations.

An average particle is made up of (a) unperturbed Pt atom layers where the "main" interatomic distances observed at 2.75 ± 0.05 Å and 3.94 ± 0.07 Å are in agreement with those observed for the

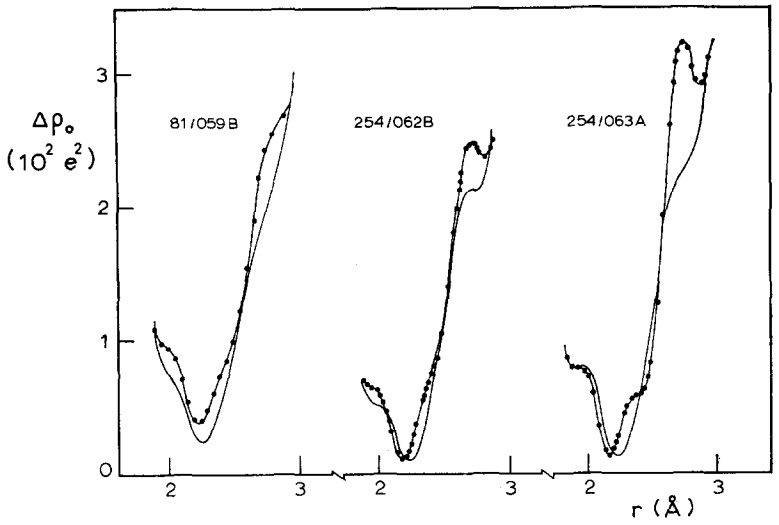

FIG. 6. Radial electron density distribution functions for the Pt supported catalysts (——) and the corresponding support (—).

bulk metal, the coordination number for the first distance being $Z = 12$, and (b) perturbed Pt atom layers, approximately 2 in number. In the prereduced catalysts, exposed to the ambient atmosphere, the coordination number of Pt in these layers is zero suggesting a complete disorder. The 1:1 Pt–O stoichiometry permits such a disorder. In the reduced catalyst kept in H_2 (reduced *in situ*), the coordination number of Pt in these perturbed layers is close to 6, i.e., $Z/2$.

TABLE 2
SOME INTERATOMIC VECTORS USED IN THE RED CALCULATIONS

Vector[c]	Distance, Å
Si–O	1.62[a]
Al^{IV}–O	1.75[b]
Al^{VI}–O	1.90[b]
O–O	2.65[a]
Al^{VI}–Al^{VI}	2.79[b]
Si–Si	3.12[a]
Al^{IV}–Al^{VI}	3.276[b]
Al^{IV}–Al^{IV}	3.421[b]

[a] R. L. Mozzi and B. E. Warren, *J. Appl. Crystallogr.* **2**, 164 (1969).

[b] A. J. Léonard, P. N. Semaille, and J. J. Fripiat, *Proc. Brit. Ceram. Soc.* 103 (1969).

[c] Al^{IV} or Al^{VI} represent, respectively, fourfold and sixfold coordinated aluminium atoms.

Objections may be raised to the use of the RED technique in that it does not provide information on "good" catalysts since the amplitude of the Pt peaks decreases as the dispersion increases. From this work it is clear that the "average Pt particle" corresponding to dispersion degree of up to about 70% provokes a deformation of the radial electron distribution obtained for the support alone and that information about the order–disorder in the Pt arrangement can be derived from it. However, and this is true

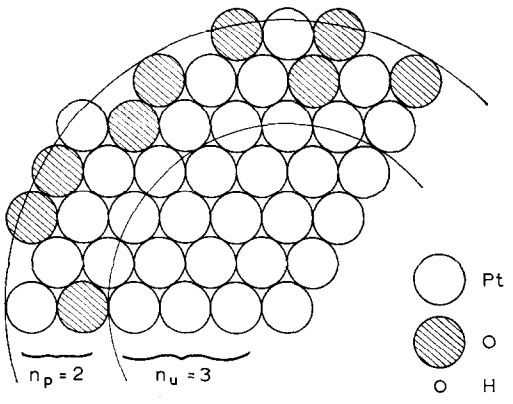

FIG. 7. Model used for the calculation of the dispersion degree [Eq. (5)]. The circles representing the Pt, O, and H atoms have radii of metal platinum, ionic oxygen and covalent hydrogen.

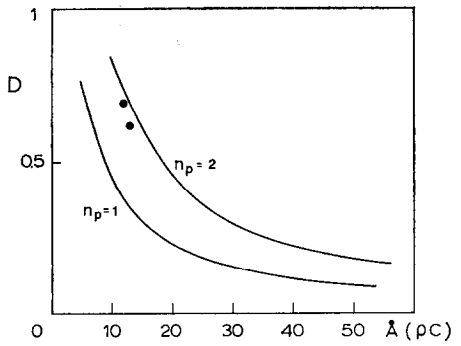

FIG. 8. Solid lines: D vs ρC according to Eq. (5). The two experimental points were obtained for catalysts 366, B and C (see Table 1).

for almost any physical technique applied to catalysis, it must again be emphasized that it is only through the simultaneous use of various physical and chemical methods of investigation that coherent information can be obtained. From this viewpoint the good agreement between the RED peak amplitude and the dispersion degree is encouraging.

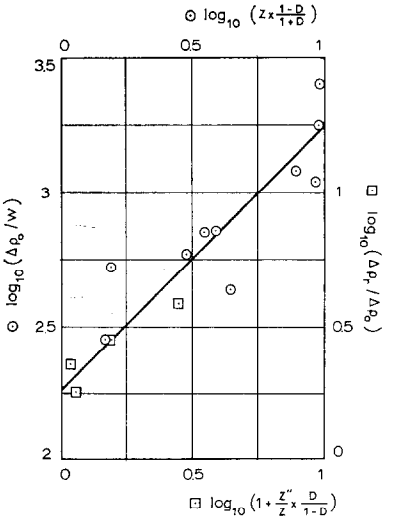

FIG. 9. Circle: variation of the amplitude of the RED peak corresponding to the Pt–Pt 2.75 Å ± 0.05 Å interatomic vector as suggested by Eq. (6) for $Z' = 0$ for the prereduced catalysts. Square: variation of the ratio of the amplitude of the same RED peak after reduction *in situ* to the amplitude obtained for the prereduced catalyst as suggested by Eq. (7).

ACKNOWLEDGMENTS

We are grateful to Messers H. Debus, M. Van Tongelen, R. Cahen, and J. André of Labofina, for supplying the catalysts as well as the platinum dispersion values.

We wish to express our appreciation to Professors Meinguet and Debroux of the Computer Centre of the University for the tedious numerical calculations involved in this work.

Our thanks are due to Dr. G. L. Haller for reading through the manuscript and suggesting valuable changes.

We are also grateful to Messers C. Defossé and M. Genet for technical assistance.

This work was sponsored by "Institut pour l'Encouragement de la Recherche Scientifique dans l'Industrie et l'Agriculture (I.R.S.I.A.)" and by Labofina S.A.

REFERENCES

1. BOUDART, M., *Adv. Catal.* **20**, 153 (1969).
2. RATNASAMY, P., AND LÉONARD, A. J., *Catal. Rev.* **6** (2), 293 (1972).
3. BENSON, J. E., AND BOUDART, M., *J. Catal.* **4**, 704 (1965).
4. ANDERSON, J. R., AND AVERY, N. R., *J. Catal.* **5**, 446 (1966).
5. LÉONARD, A. J., RATNASAMY, P., DECLERCK, F. D., AND FRIPIAT, J. J., *Disc. Faraday Soc.* **52**, 98 (1971).